

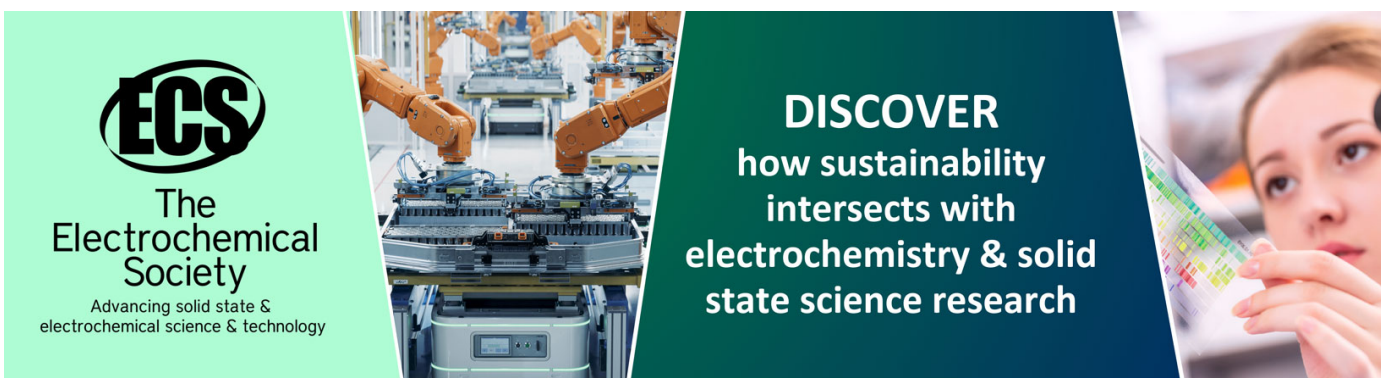
Direct electron transfer of glucose oxidase on carbon nanotubes

To cite this article: Anthony Guiseppi-Elie *et al* 2002 *Nanotechnology* **13** 559

View the [article online](#) for updates and enhancements.

You may also like

- [Amperometric Glucose Biosensor Based on Glucose Oxidase, 1,10-Phenanthroline-5,6-dione and Carbon Nanotubes](#)
Erhan Zor, Yasemin Oztekin, Almira Ramanaviciene et al.
- [Formation and Electrochemical Characterisation of Enzyme-Assisted Formation of Polypyrrole and Polyaniline Nanocomposites with Embedded Glucose Oxidase and Gold Nanoparticles](#)
Natalija German, Anton Popov, Almira Ramanaviciene et al.
- [Enhancement of Glucose Oxidase-Based Bioanode Performance by Comprising *Spirulina platensis* Microalgae Lysate](#)
Rokas Žalnavičius and Arunas Ramanavicius



ECS
The
Electrochemical
Society
Advancing solid state &
electrochemical science & technology

DISCOVER
how sustainability
intersects with
electrochemistry & solid
state science research

Direct electron transfer of glucose oxidase on carbon nanotubes

Anthony Guiseppi-Elie^{1,3}, Chenghong Lei¹ and Ray H Baughman²

¹ Department of Chemical Engineering and Center for Bioelectronics, Biosensors and Biochips, (C3B), Virginia Commonwealth University, PO Box 843038, 601 West Main Street, Richmond, VA 23284-3038, USA

² Research Technology Center, Honeywell Corporation, Morristown, NJ 07962, USA

E-mail: guiseppi@vcu.edu

Received 25 March 2002, in final form 22 July 2002

Published 30 August 2002

Online at stacks.iop.org/Nano/13/559

Abstract

In this report, exploitation of the unique properties of single-walled carbon nanotubes (SWNT) leads to the achievement of direct electron transfer with the redox active centres of adsorbed oxidoreductase enzymes. Flavin adenine dinucleotide (FAD), the redox active prosthetic group of flavoenzymes that catalyses important biological redox reactions and the flavoenzyme glucose oxidase (GOx), were both found to spontaneously adsorb onto carbon nanotube bundles. Both FAD and GOx were found to spontaneously adsorb to unannealed carbon nanotubes that were cast onto glassy carbon electrodes and to display quasi-reversible one-electron transfer. Similarly, GOx was found to spontaneously adsorb to annealed, single-walled carbon nanotube paper and to display quasi-reversible one-electron transfer. In particular, GOx immobilized in this way was shown, in the presence of glucose, to maintain its substrate-specific enzyme activity. It is believed that the tubular fibrils become positioned within tunnelling distance of the cofactors with little consequence to denaturation. The combination of SWNT with redox active enzymes would appear to offer an excellent and convenient platform for a fundamental understanding of biological redox reactions as well as the development of reagentless biosensors and nanobiosensors.

1. Introduction

Since the discovery of carbon nanotubes (CNT) by Iijima in 1991 [1], there has been an explosion of research into the physical and chemical properties of this novel material [1–10]. Considerable interest in demonstrating unique uses for these materials is now emerging. Recently, Baughman *et al* [10] reported that electromechanical actuators based on sheets of single-walled carbon nanotubes (SWNT), serving as electrodes, could generate higher stresses than natural muscle and higher strains than high-modulus ferroelectrics [10]. Based on the fullerene structure of graphitic sheets seamlessly wrapped into cylinders, SWNT display excellent chemical stability, good mechanical strength and a range of electrical conductivity [1–8]. CNT may therefore be ideal electrode/nanoelectrode materials. The similarity in

length scales between nanotubes and redox enzymes suggests interactions that may be favourable for biosensor electrode applications. Not least among the important characteristics of SWNT are their inherent high surface area and tubular structure. The purification of SWNT with oxidizing acids such as nitric acid also inevitably creates surface acid sites that are mainly carboxylic and possibly phenolic on both the internal and external surfaces of the oxidized nanotubes [7, 8, 10–13]. The high surface area possessing abundant acidic sites may offer special opportunities for the adsorption and entrapment of chemical/biological molecules [11–16].

The immobilization of DNA, proteins and enzymes onto CNT, the helical crystallization and the interaction of proteins with CNT leading to the development of new biosensors have been reported [11–17]. In these latter reports the CNT appeared to act as benign hosts to trap and support the biological molecules, and the surface acidic sites may have

³ Author to whom any correspondence should be addressed.

served to enhance the binding of the biomolecules. However, there was no apparent direct electronic communication between the CNT and the biological molecules. Within living cells [18], the many redox proteins and enzymes that are part of the electron transport chain are located on or are supported by biological membranes. The resulting proximity and control of spatial orientation, one to the other, greatly facilitates the energetics and kinetics of the redox processes. Direct electrochemical reactions of redox proteins and redox enzymes at solid state electrodes may bring new insights into the biological electron transfer processes [19] as well as enable new classes of reagentless biosensors. The direct electrochemistry of the heme proteins and flavo enzymes has been widely investigated since the 1970s. However, in the absence of mediating small molecules, well-defined direct electrochemical behaviour of flavoprotein-oxidase systems is rendered extremely difficult as the flavin adenine dinucleotide (FAD) moiety is deeply embedded within a protective protein shell. Binding of the prosthetic group to the apo-protein is believed to cause steric hindrance to electron exchange with the electrode [20]. Through physical adsorption or direct covalent immobilization of biomolecules [11–17], CNT with the aforementioned combined physico-chemical characteristics could open up a new approach to direct electrical communication with redox active biomolecules.

2. Discussion

The SWNT used in this work were commercially supplied (Nanotubes at Rice) and were made by the dual pulsed-laser vaporization method and the purification process involved nitric acid reflux, cycles of washing and centrifugation, and finally cross-flow filtration [7, 8, 10]. The materials prepared in this way comprise hexagonally packed bundles of CNT that have diameters of 12–14 Å, an intertube separation within a bundle of ~17 Å, an average bundle diameter of ~100 Å and tube lengths of many micrometres. In one instance, the aqueous suspension of SWNT was cast as thin films onto glassy carbon electrodes (GCE) (SWNT/GCE). In another instance, free-standing single-walled CNT papers (SWNTP) were formed by vacuum filtration and washing of the nanotube suspension. Sheets of the dried nanotube paper were peeled from the filter and annealed in an inert atmosphere [7, 8, 10]. The GCE support is not suited to the high-temperature (500 °C) annealing conditions used for the SWNT paper. The GCE is fundamentally different from CNT in structure and is vulnerable to oxidation at these temperatures. Also, the GCE electrodes are encapsulated in an epoxy resin that would not withstand these annealing conditions. Therefore, no experiments were performed using annealed SWNT/GCEs as electrodes.

Figure 1(a) shows the dramatic change of the cyclic voltammogram (CV) obtained in a pH 7.0, 33 mM phosphate buffer containing 0.1 M KCl and 0.1 mM FAD at GCE and at SWNT/GCE respectively. The peak current of the electroactive FAD at SWNT/GCE (dashed curve) is almost 22 times as large as that found at the bare GCE (dot/dash mixed curve). This indicates a much larger effective working electrode area of SWNT/GCE compared with GCE alone. The observation that there is no difference in the shape of the CV indicates that there are no unusual influences of the

SWNT–GCE interface that may be attributable to electron transfer between the SWNT and the GCE support. Upon removal of the SWNT/GCE working electrode from the test solution of FAD, the electrode was rinsed thoroughly with the buffer and the CVs were again obtained in FAD-free buffer solution. These CVs are shown in figure 1(a) (dotted curve and solid curve) and at multiple scan rates in figure 1(b). FAD adsorbed onto the SWNT/GCE (FAD/SWNT/GCE) displayed a well-defined CV with a formal potential of –448 mV (all potentials versus Ag/AgCl). The small redox peak separation (ΔE_p) changed from 18 mV at 10 mV s⁻¹ through 36 mV at 50 mV s⁻¹ to 56 mV at 140 mV s⁻¹. The corresponding peak width at half-height changed from 76 mV at 10 mV s⁻¹ to 82.5 mV at 50 mV s⁻¹ through to 92 mV at 140 mV s⁻¹. These observations indicate that the adsorbed FAD displayed a quasi-reversible one-electron transfer process on SWNT. Furthermore, the linear relationship of the peak current with the scan rate demonstrates that the electron transfer of the adsorbed FAD was typical for a surface-confined electrode reaction. The electron transfer rate of FAD/SWNT/GCE was determined by the method of Laviron [21] and found to be 3.1 s⁻¹.

SWNT/GCE that was incubated overnight at 4 °C in glucose oxidase (GOx) solutions resulted in spontaneous adsorption of the enzyme onto the unannealed SWNT (GOx/SWNT/GCE) and displayed the electroactivity shown in figure 1(c) (solid curve). While the CV shows clear evidence of electroactivity that was exactly coincident with that of the adsorbed FAD (dotted curve), the ratio of peak current to the electrode capacity current was much less than that of adsorbed FAD. The large separation between the anodic and cathodic base currents that establishes a large CV envelope area indicates capacitive charging of the electrified interface in the presence of the adsorbed protein. This suggests that under the present conditions, either the globular protein shell of GOx was still an obstacle for the direct electron transfer of the enzyme to the electrode or that the enzyme loading onto such unannealed SWNT/GCE was very limited. As shown later, the AFM evidence refutes this latter possibility.

Similarly, FAD and GOx were also adsorbed onto freestanding carbon nanotube paper (SWNTP) in both its unannealed and annealed forms. FAD and GOx adsorbed on unannealed SWNTP displayed similar CVs to those obtained on unannealed SWNT/GCE, while the electrochemical behaviours of FAD and GOx on annealed SWNTP were totally and dramatically different. The similarity of electrode responses of unannealed SWNT/GCE with adsorbed FAD and of freestanding annealed SWNTP with adsorbed GOx indicates that the GCE support had little or no influence on the overall electrochemical behaviour of the SWNT. On the other hand, the difference in behaviour of FAD and GOx on annealed SWNTP indicates that the annealing step is an important contributor to electrochemical behaviour.

Figure 2(a) shows the CV of FAD adsorbed onto annealed SWNTP. FAD adsorbed on the annealed SWNTP displayed an unsymmetrical CV and rather large ΔE_p values (85 mV at 10 mV s⁻¹, 146 mV at 50 mV s⁻¹ and 207 mV at 140 mV s⁻¹). FAD adsorbed in this way (FAD/SWNTP) displayed an irreversible transfer process, a dramatic change when compared with that of FAD adsorbed on SWNT/GCE made from the aqueous suspension of unannealed CNT (see

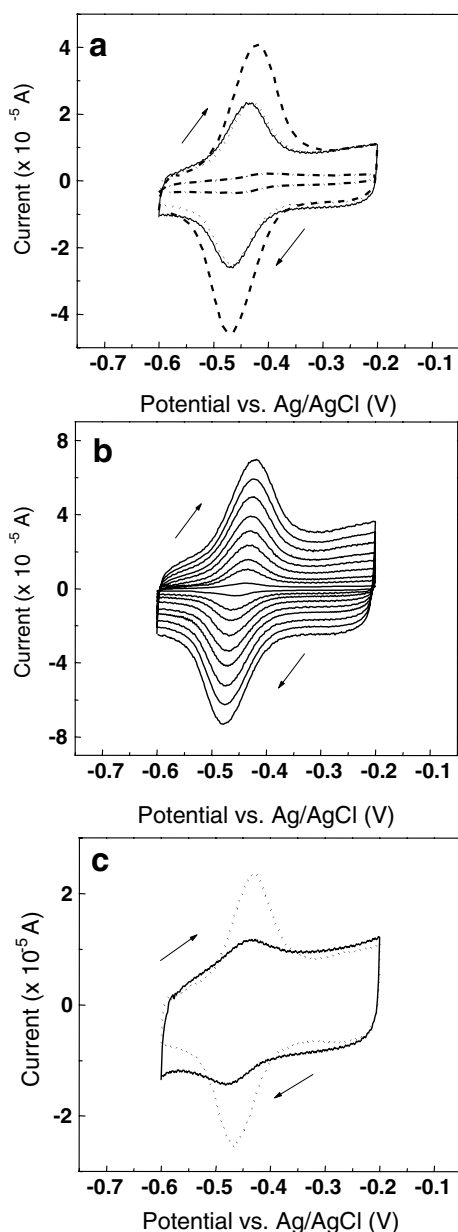


Figure 1. CV of FAD and GOx adsorbed on SWNT/GCE. (a) GCE in pH 7.0 phosphate buffer/0.1 M KCl containing 0.1 mM FAD (dot/dash mixed curve); SWNT/GCE in pH 7.0 phosphate buffer/0.1 M KCl containing 0.1 mM FAD (dashed curve); FAD/SWNT/GCE in pH 7.0 phosphate buffer/0.1 M KCl (dotted curve); FAD/SWNT/GCE in pH 7.0 phosphate buffer/0.1 M KCl after leaving overnight (solid curve). Scan rate: 50 mV s^{-1} . (b) FAD/SWNT/GCE in pH 7.0 phosphate buffer/0.1 M KCl at the scan rates (mV s^{-1}) of: 10, 25, 35, 50, 65, 80, 100, 120, 140 (from inner to outer). (c) GOx/SWNT/GCE in pH 7.0 phosphate buffer/0.1 M KCl (solid curve); FAD/SWNT/GCE in pH 7.0 phosphate buffer/0.1 M KCl (dotted curve). Scan rate: 50 mV s^{-1} .

figure 1(b)). The electron transfer rate of FAD/SWNT/GCE was as low as 0.38 s^{-1} when determined using the method of Laviron [21]. This observed change may be caused by FAD overloading due to the larger active surface area of the annealed CNT. The unannealed SWNT formulation contains about 30% additives (particularly surfactants), which might decrease the effective or active surface area of the nanotubes so that the overloading of FAD was avoided in the case of

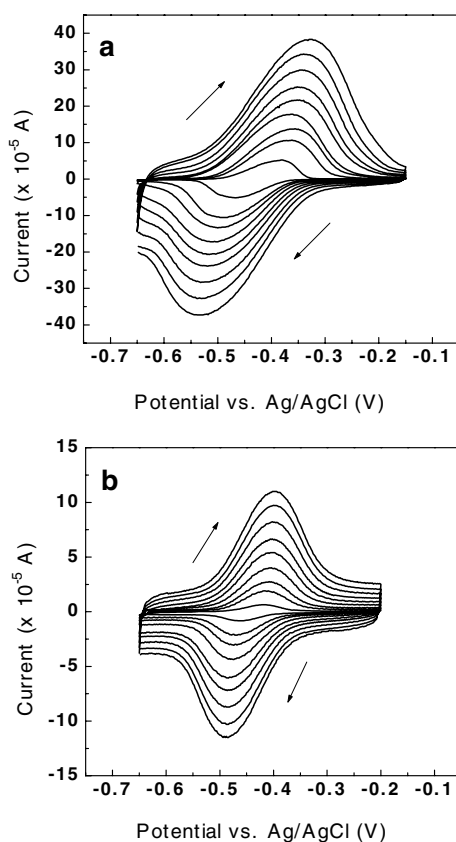


Figure 2. CV of FAD (a) and GOx (b) adsorbed on annealed SWNT/GCE in pH 7.0 phosphate buffer/0.1 M KCl at the scan rates (mV s^{-1}) of 10, 25, 35, 50, 65, 80, 100, 120, 140.

the results shown in figure 1. On the other hand, figure 2(b) shows the CV of GOx adsorbed on the annealed SWNT/GCE. There is a significant increase in measured electroactivity when compared with that on the unannealed SWNT/GCE (not shown) and SWNT/GCE (shown in figure 1(c)). Unlike FAD, GOx adsorbed on the annealed SWNT/GCE (GOx/SWNT/GCE) displayed almost symmetrical CV shapes with equal reduction and oxidation peak heights and with a formal potential of -441 mV . The peak potential of GOx/SWNT/GCE is close to that of FAD, indicating that the electroactivity of the adsorbed GOx on annealed SWNT/GCE did result from the FAD moiety of the enzyme molecule. Multiple scan rate cyclic voltammetry (MSRCV) of the GOx/SWNT/GCE shows that the redox peak separation changed from 43 mV at 10 mV s^{-1} , through 71 mV at 50 mV s^{-1} , to 87.5 mV at 140 mV s^{-1} . The corresponding peak width at half-height changed from 74 mV at 10 mV s^{-1} , through 109 mV at 50 mV s^{-1} , to 124 mV at 140 mV s^{-1} . Obviously, like FAD/SWNT/GCE, the adsorbed GOx on the annealed SWNT/GCE (GOx/SWNT/GCE) also displayed a quasi-reversible one-electron transfer process. The linear relationship of the peak current with the scan rate likewise shows that the adsorbed GOx performed as a surface-confined electrode reaction. The electron transfer rate of GOx/SWNT/GCE was found to be 1.7 s^{-1} when determined by the method of Laviron [21]. This value is lower than that found for FAD/SWNT/GCE because of the steric hindrance arising from the association of FAD with the apo-protein component of the enzyme.

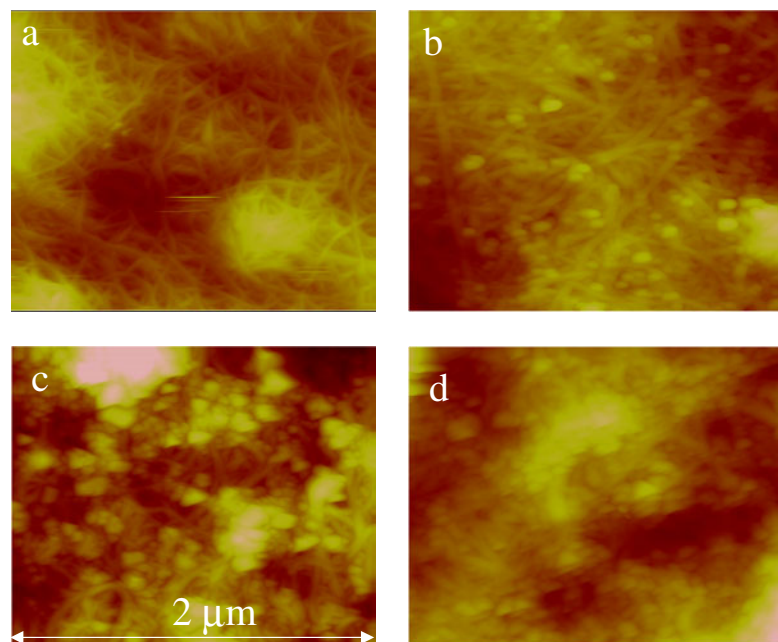


Figure 3. AFM tapping-mode images (height profiles) of GOx adsorbed on SWNT. (a) The annealed SWNT. (b) GOx on the annealed SWNT. (c) The unannealed SWNT. (d) GOx on the unannealed SWNT.

(This figure is in colour only in the electronic version)

These results demonstrate that after annealing, the elegantly simple physico-chemical adsorption of GOx to the surface of the annealed SWNT results in direct electron transfer to the cofactor of the enzyme. Moreover, the enzyme loading was large enough to support readily detectable redox currents. Figure 3 shows the images, obtained by atomic force microscopy (AFM), of GOx adsorbed on both the annealed SWNT and the unannealed SWNT⁴. The surfactant molecules, shown as aggregates on the unannealed SWNT in figure 3(c), were removed during the high-temperature annealing process (compare figures 3(a) and (c)). It is also very clear that the globular protein (GOx) molecules were adsorbed on the larger available surface area of ‘clear’ annealed SWNT (see figures 3(a) and (b)). The unannealed SWNT also allowed considerable adsorption of GOx (see figures 3(c) and (d)). At a glance, the unannealed SWNT appears to have globular adsorbates (about 10–20 nm) that resemble the globular features found on GOx/SWNT. Furthermore, the unannealed SWNT, after being exposed to GOx, is more densely covered by these globular features but displays less GOx-related electroactivity. This arises, we believe, because the adsorbed surfactant effectively prevents access to those features that enable direct electroactivity of GOx at the SWNT surface.

There is little doubt that the active surface area of CNT increases dramatically after annealing; the MSRCV data with FAD confirms this view. More importantly, the resulting surfaces allowed direct electron transfer to adsorbed GOx. It is believed that nanoscale ‘dendrites’ of CNT project outwards from the surface and act like bundled ultra-microelectrodes that allow access to the active site and permit direct electron transfer

⁴ AFM tapping-mode images (height profiles) were taken with *Digital Instruments Nanoscope III* atomic force microscope (Digital Instruments, USA).

to the adsorbed enzyme. In other words, during the adsorption of GOx, the protein confers its surfactant-like qualities to the surface of the annealed SWNT and in so doing the protein adsorption permits small assemblies of CNT (possibly individual nanotubes) to approach and be physically located within the electron tunnelling distance of the prosthetic group FAD of the enzyme. Thus, the SWNT surface, because of its nanostructured topology, allows the enzyme to be adsorbed and the electrode to be positioned close to the electroactive prosthetic group. The elegant simplicity arises because the electrode structure and the enzyme both share the same length scale. The enzyme is able to be adsorbed onto the surface of the SWNT without losing its overall biological shape, form and/or function. The present results suggest the analogy of piercing a balloon with a long sharp needle such that the balloon does not pop. Instead, by a gentle twisting action the needle can be made to enter the balloon without the balloon losing its integrity or its air. The needle, once having pierced the outer skin of the balloon could now interact with the contents of the balloon. In this way, some number of SWNTs are able to ‘pierce’ the glycoprotein shell of the GOx and gain access to the redox sites and be established within tunnelling distance of the redox active co-factor (FAD) of the enzyme. This then will allow direct electron transfer. Such access is not generally accorded to the smooth, polished surfaces of traditional electrodes.

However, did the adsorbed GOx, while demonstrating electroactivity at the SWNT surface, still retain its glucose-specific enzyme activity? Shown in figure 4 is confirmatory evidence that GOx adsorbed onto the annealed SWNT, while directly electroactive, still retained its enzyme specific activity and was responsive to glucose. Figure 4(a) shows the CV obtained in oxygen-free buffer solution (solid curve, also see figure 2(b)), which was later re-aerated to oxygen-saturation and another CV obtained (dotted curve). Under

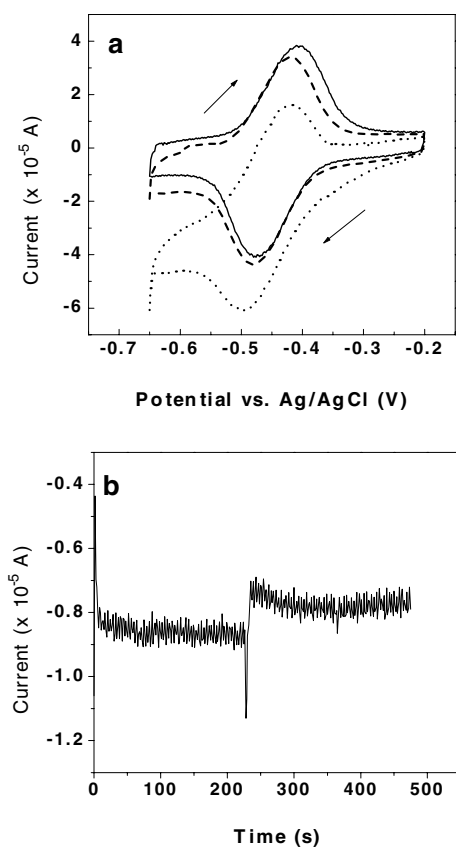


Figure 4. Electrochemical detection of enzyme activity of GOx adsorbed on annealed SWNT. (a) CV of GOx adsorbed on annealed SWNT in the O_2 -free pH 7.0 phosphate buffer/0.1 M KCl (solid curve); in the O_2 -saturated buffer (dotted curve); and after addition of glucose to the final concentration of 25 mM (dashed curve). Scan rate: 50 mV s^{-1} . (b) Chronoamperometric record of GOx adsorbed on annealed SWNT in O_2 -saturated pH 7.0 phosphate buffer/0.1 M KCl at a constant potential of -475 mV while glucose was added at 226 s to a final concentration of 25 mM.

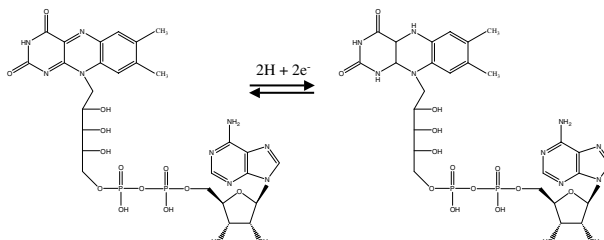
these conditions the catalytic reduction peak current for oxygen ($2\text{FAD} + \text{O}_2 \rightarrow 2\text{FAD}^+ + \text{O}_2^{2-}$) is clearly observed as the dotted curve. Next, a chronoamperometric experiment at a constant potential of -475 mV was carried out under constant stirring. Upon the addition of glucose, the monitored current was dramatically increased as shown in figure 4(b). This is in agreement with the subsequent CV that shows an almost perfect return to the oxygen-free condition (the dashed curves in figure 4(a)) as the presence of glucose promotes the consumption of oxygen. These results demonstrate that molecular oxygen was consumed at the electrode interface ($\text{glucose} + \text{O}_2 \rightarrow \text{gluconolactone} + \text{H}_2\text{O}_2$) and accordingly confirms that the oxidase still maintained its specific enzyme activity. Two months later, both the electroactivity and the apparent enzyme activity were still measurable at about 70% of the initial value.

We have demonstrated that CNT, when combined with a member of the important family of oxidase enzymes such as GOx, offer the opportunity for research of the electron transfer chemistry of these biological redox molecules. This system also allows external potentiation of redox enzyme/protein activity for biological reaction engineering as well as the construction of novel biosensors and nanobiosensors. Our work is now directed to covalent immobilization of cofactors

and oxidoreductases to the acid sites of single CNTs for the construction of nanobiosensors that could be used in the study of sub-cellular kinetics.

Experimental details

Flavin adenine dinucleotide (FAD, Product No: F-6625) and GOx (GOx, Product No: G-7016) were obtained from



Sigma. GOx (1-oxidoreductase, EC 1.1.3.4) is a FAD-dependent enzyme that catalyses the oxidation of β -D-glucose by molecular oxygen. The working solution of pH 7.0, 33 mM phosphate buffer containing 0.1 M KCl was prepared as usual. Aliquots ($10 \mu\text{l}$) of 0.4 g l^{-1} aqueous suspension of SWNT were deposited on GCE (GCE, 3 mm diameter) and allowed to dry under ambient conditions to form SWNT-modified electrodes (SWNT/GCE). A certain area of carbon nanotube paper (SWNT, unannealed and annealed) was also used as working electrodes. The resulting electrodes were sequentially rinsed with water, methanol, water and the working buffer just before carrying out CV experiments in 0.1 mM FAD or being incubated overnight at 4°C in $100 \mu\text{l}$ of the working buffer containing 2 mg of GOx. FAD or GOx was thus spontaneously adsorbed onto the SWNT electrodes. Modified electrodes were rinsed completely with the working buffer solution prior to use and so the following electrode constructs were obtained: FAD/SWNT/GCE, GOx/SWNT/GCE, FAD/SWNT and GOx/SWNT. All electrochemical experiments were carried out at $20 \pm 1^\circ\text{C}$ using a computer-controlled EG&G Potentiostat/Galvanostat Model 273 (Princeton Applied Research). The electrochemical cell was equipped with a working electrode as described above, a Ag/AgCl (3.0 M NaCl) reference electrode and a platinum wire counter electrode. Prior to measurement, 4 ml of 33 mM phosphate buffer containing 0.1 M KCl was carefully bubbled with argon for at least 20 min to remove oxygen. The CNTP was first heated to 150°C in a convection oven to remove residual solvent and then transferred to a tube furnace and annealed at $10^\circ\text{C min}^{-1}$ from ambient to 450°C while purging in an argon atmosphere. AFM tapping-mode images (height profiles) were taken with a Digital Instruments Nanoscope III atomic force microscope (Digital Instruments, USA).

Acknowledgments

We thank the financial support of the VCU Center for Bioelectronics, Biosensors and Biochips, the Virginia Center for Innovative Technology (CIT BIO-99-010) and the NSF (DGE 9902567).

References

- [1] Iijima S 1991 *Nature* **354** 56
- [2] Buongiorno Nardelli M, Fattebert J-L, Orlikowski D, Roland C, Zhao Q and Bernholc J 2000 *Carbon* **38** 1703
- [3] Wong E W, Sheehan P E and Lieber C M 1997 *Science* **277** 1971
- [4] Yakobson B I and Smalley R E 1997 *Am. Sci.* **85** 324
- [5] Mintmire J W, Dunlap B I and White C T 1992 *Phys. Rev. Lett.* **68** 631
- [6] Chopra N, Benedict L, Crespi V, Cohen M L, Louie S G and Zettl A 1995 *Nature* **377** 135
- [7] Thess A, Lee R, Nikolaev P, Dai H, Petit P, Robert J, Xu C, Hee Lee Y, Kim S G, Rinzler A G, Colbert D T, Scuseria G E, Tománek D, Fischer J E and Smalley R E 1996 *Science* **273** 483
- [8] Liu J, Rinzler A G, Dai H, Hafner J H, Bradley R K, Boul P J, Lu A, Iverson T, Shelimov K, Huffman C B, Rodriguez-Macias F, Shon Y-S, Lee T R, Colbert D T and Smalley R E 1998 *Science* **280** 1253
- [9] Bezryadin A, Verschueren A R M, Tans S J and Dekker C 1998 *Phys. Rev. Lett.* **80** 4036
- [10] Baughman R H, Cui C, Zakhidov A A, Iqbal Z, Barisci J N, Spinks G M, Wallace G G, Mazzoldi A, De Rossi D, Rinzler A G, Jaschinski O, Roth S and Kertesz M 1999 *Science* **284** 1340
- [11] Davis J J, Green M L H, Hill H A O, Leung Y C, Sadler P J, Sloan J, Xavier A V and Tsang S C 1998 *Inorg. Chim. Acta* **272** 261 and references therein
- [12] Guo Z, Sadler P J and Tsang S C 1998 *Adv. Mater.* **10** 701
- [13] Dong L, Fischer A B, Lu M, Martin M T, Moy D and Simpson D 1996 *J. Mol. Recognit.* **9** 383
- [14] Matyshevska O P, Karlash A Y, Shtogun Y V, Benilov A, Kirgizov Y, Gorchinsky K O, Buzaneva E V, Prylutsky Y I and Scharff P 2001 *Mater. Sci. Eng. C* **15** 249
- [15] Chen R J, Zhang Y, Wang D and Dai H 2001 *J. Am. Chem. Soc.* **123** 3838
- [16] Davis J J, Green M L H, Hill H A O, Leung Y C, Sadler P J, Sloan J, Xavier A V and Tsang S C 1998 *Inorg. Chim. Acta* **272** 261
- [17] Balavoine F, Schultz P, Richard C, Mallouh V, Ebbesen T W and Mioskowski C 1999 *Angew. Chem., Int. Ed.* **38** 1912
- [18] Kotyk A, Janacek K and Koryta J 1988 *Biophysical Chemistry of Membrane Function* (Chichester: Wiley)
- [19] Frew J E and Hill H A O 1988 *Eur. J. Biochem.* **172** 261
- [20] Dryhurst G, Kadish K M, Scheller F W and Renneberg R 1982 *Biological Electrochemistry* (New York: Academic)
- [21] Laviron E 1979 *J. Electroanal. Chem.* **101** 19 and references therein